Estimating Transfer Functions with SigLab

Accurate transfer function estimation of linear, noise-free, dynamic systems is an easy task for SigLab™. Often, however, the system being analyzed is noisy or not perfectly linear. All real-world systems suffer from these deficiencies to some degree, but control systems are usually the worst offenders. Obtaining an accurate transfer function estimation from a noisy and non-linear system requires an understanding of measurement tradeoffs.

Overview

Imperfections in dynamic systems

SigLab is routinely used to estimate transfer functions associated with dynamic systems including control systems. The first half of this application note addresses the task of making accurate transfer function estimates on dynamic systems which are both noisy and non-linear. The second half covers measurement techniques focused specifically on control systems.

Electro-mechanical control systems typically are noisier and less linear than the typical electrical or purely mechanical systems. The non-linear behavior is often due to the electro-mechanical components involved in the systems. The measurement noise is often a result of the systems being characterized under actual operating conditions.

The head positioning servo of a disk drive is a good example of such a control system. The dynamics of this system are usually measured under closed-loop conditions with the disk media spinning. The mechanical imperfections of the servo track and platter inject both periodic and random signals to the control system.

In the disk drive, the non-linear behavior is primarily due to the head position error signal. In order to characterize the servo dynamics, SigLab injects a test signal into the servo system. The head position error signal has a limited linear region. As the head is driven further off its target track by this test signal, the position error signal response to the test signal becomes increasingly non-linear. The end result of this combined noise and non-linearity is a measurement challenge.

Balancing noise and non-linearity

To make a transfer function measurement on a dynamic system, an excitation is supplied to the system and the system's response to this excitation is measured. If the system is noisy but linear, the excitation level can be increased to improve the signal to noise ratio by simply overpowering the noise. If the system non-linear at high excitation amplitudes, but free of noise, the excitation can be lowered to a point where the linearity is acceptable.

When the system is both non-linear and noisy, a tradeoff must be made balancing the poor signal-to-noise ratio at low excitation amplitudes with the non-linear system behavior at high excitation amplitudes.

Two primary tools for transfer function estimation

SigLab comes with two software applications for transfer function estimation: swept-sine and a broad-band FFT based network analyzer.

The swept-sine (or more accurately stepped-sine) estimation technique is the least affected by noise and non-linear system behavior. The main tradeoff with the swept-sine technique is measurement time. The transfer function is estimated over a user-defined frequency range a single frequency point at a time.

In measurement situations where there is reasonable linearity and good signal to noise ratio, SigLab's broad-band FFT based network analyzer provides the transfer function estimate in a fraction of the time that is normally needed by the swept-sine approach. The excitation is usually a bandlimited random or periodic chirp signal, but, the user is not limited to these excitations. A signal selection from the function generator application or an external source, may be used.

The following five factors have the most impact on the amount of time required for a transfer function estimate:

1) system's noise
2) system's linearity
3) number of frequencies points in the estimate
4) required accuracy
5) required frequency resolution

Measurement Configurations

The optimal measurement configuration

The goal is to determine the system transfer function $H(w)$ from measurements on the system. The optimal measurement configuration for the Device Under Test (DUT) and SigLab is shown in Figure 1. At this point, no assumptions are being made about the type of system being measured. It could be purely electrical, electro-mechanical, mechanical, acoustical, and so on.

The measurement configuration in Figure 1 assumes that the excitation $x(t)$ can be measured with minimal error. If SigLab's output source is directly connected to both the DUT input and a SigLab input, this is a perfectly valid assumption.

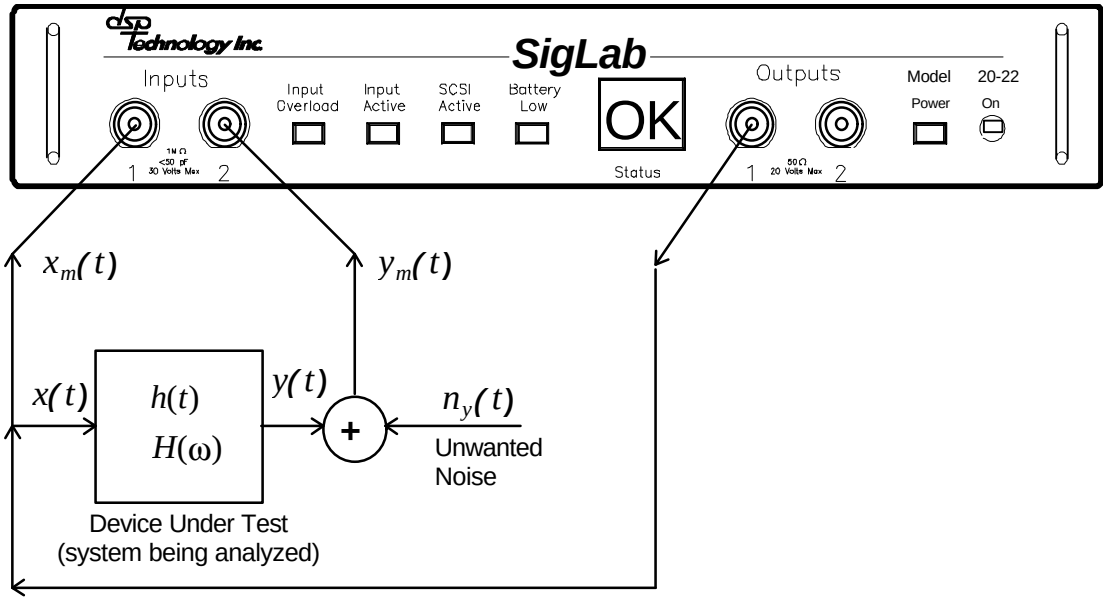

Figure 1 - Optimal SigLab Measurement Configuration

However, Figure 1 assumes that the excitation to the system is a voltage, but this is often not the case in mechanical or electro-mechanical work. A transducer must be used to convert the system's excitation into a voltage which can then be measured with SigLab. For instance, a force-to-voltage transducer can be used to measure the input excitation force to a mechanical system. In these cases, precautions must be taken to insure that minimal electrical noise corrupts the signal from the transducer and that the transducer is operated in its linear region. When these precautions are observed, the assumption that the system's excitation can be measured with minimal error is still valid.

Therefore, as shown in Figure 1, the entire measurement uncertainty is accounted for in the DUT's response signal $y_m(t)$ by the additional (unwanted) noise term $n_y(t)$. When the excitation to the system is zero, the response, $y(t)$, of the system is zero, and therefore $y_m(t) = n_y(t)$. There are no other assumptions about the character of this noise.

It is important to recognize that the measurement noise term $n_y(t)$ is usually not provided by an actual external noise source. It simply represents the system's output with no input.

At first it might seem that the assumption of having a noiseless excitation channel measurement is unreasonable. In practice, however, this requirement is usually attainable.

If an accurate measurement of the excitation to the system can be made, it is relatively easy to obtain an *unbiased* estimate of the system's transfer function. This is the ***primary reason*** for configuring the DUT and SigLab as shown in Figure 1.

The transfer function estimation, $\hat{H}(w)$, is computed from cross and auto power spectra estimates[1] as shown in (1):

$$\hat{H}(w) = \frac{\hat{P}_{xy}(w)}{\hat{P}_{xx}(w)} \qquad (1)$$

where $\hat{P}_{xy}(w)$ is the cross power spectrum between the excitation $x_m(t)$ and response $y_m(t)$ and $\hat{P}_{xx}(w)$ is the auto power spectrum of the excitation signal.

These spectral estimates ($\hat{P}_{xx}(w)$, $\hat{P}_{xy}(w)$) are computed internally to SigLab using the FFT, windowing, and frequency-domain averaging. When more averaging is specified, more data is acquired and processed to refine these estimates. SigLab's hardware and software is optimized to make these calculations in real-time.

As the amount averaging used in the computations is increased, the estimate $\hat{H}(w)$ will converge to the actual transfer function $H(w)$. This is a key property of an unbiased estimator. The amount of averaging required to attain a given accuracy for the transfer function estimate is a function of the noise $n_y(t)$: less noise, less averaging.

The coherence is an auxiliary computation often made in conjunction with the transfer function estimate. The coherence calculation in (2) provides an indication of the portion of the system's output power that is due to the input excitation.

$$\hat{C}(\omega) = \frac{\left|\hat{P}_{xy}(\omega)\right|^2}{\hat{P}_{xx}(\omega)\hat{P}_{yy}(\omega)} \qquad (2)$$

The coherence, $\hat{C}(w)$, has a range of 0.0 to 1.0, where 1.0 indicates that all of the measured output power is due to the input excitation. This, of course, is the most

desirable situation and will only be true at frequencies where the energy of the noise $n_y(t)$ is negligible. The coherence may be viewed as an indicator of measurement quality. When a significant portion of the measured output is not related to the excitation (e.g. the noise term $n_y(t)$ is large), a low coherence will result. For a given amount of averaging, the variance of the transfer function, at frequencies where the coherence is low, will be higher than the variance where the coherence is closer to 1.0.

However, since the transfer function estimate is unbiased, the estimate will eventually converge to the system's actual transfer function given sufficient averaging. This is true even if the coherence is low.

To minimize measurement time, the above transfer function and coherence estimation calculations are implemented internally in SigLab.

The broad-band FFT technique

The FFT based network analyzer computes the transfer function and coherence simultaneously over a band of frequencies using the method outlined in (1) and (2). The frequency range usually spans from dc to a user-defined upper limit. Analysis of a band of frequencies centered about a specified center frequency is also supported. In order to carry out the transfer function measurement, the excitation to the system must contain frequency components covering the selected frequency range (ergo, not a sine wave). Selecting either the chirp or random excitation from the control panel of the network analyzer application is the simplest way to meet this objective. However, if customized excitations are desired, an external source or the function generator application can be used.

The swept-sine technique

Swept-sine analysis differs from the broad-band technique in that a single frequency sine signal is used as the excitation to the system. SigLab's input data acquisition subsystem can be configured as digital tracking band-pass filters. The center frequency of these filters is set to match the frequency of the sine excitation. These band-pass filters can drastically reduce measurement noise. At the expense of measurement speed, a lower filter bandwidth may be selected, providing greater noise immunity if needed. The transfer function is still obtained by taking the ratio of the cross and auto spectra, but, now it is computed using the band-pass filtered time histories. When the transfer function estimate has been computed, the output source frequency is advanced to the next frequency desired for the transfer function estimation, and the measurement is repeated. The swept-sine uses:

- single frequency excitation
- tracking digital band-pass filters
- unbiased cross-auto transfer function estimator

thereby providing an accurate transfer function estimate under the most demanding measurement conditions.

Some Measurement Examples

The linear/noise-free measurement

Figure 2 shows a transfer function estimate, made by the broad-band FFT based network analyzer, on a linear, noise free, dynamic system. SigLab is connected to the DUT as shown in Figure 1.

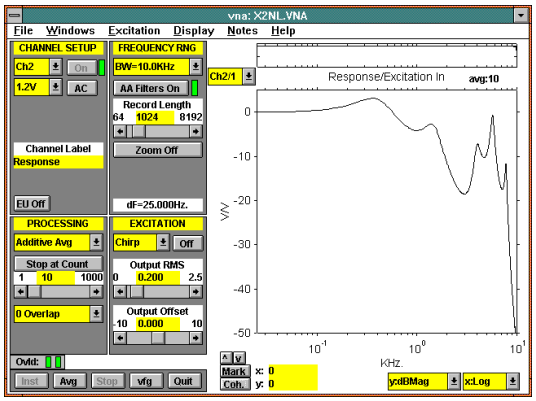

Figure 2 - Transfer Function of a linear, noise-free system.

The transfer function is measured simultaneously at 401 discrete frequency points over the dc-10 kHz range therefore providing a 25 Hz frequency resolution. The magnitude of the transfer function, in dB, is plotted on the y-axis with a logarithmic frequency x-axis. The total measurement time was well under 1 second.

The coherence is plotted on the axis above the transfer function estimate. Only ten averages were used to make the measurement since the system is virtually noise-free. In fact, little or no averaging was actually required to obtain an excellent transfer function estimate, however, the coherence calculation is not meaningful unless there is some amount of averaging.

Measurements on a noisy, but linear, system

The next example demonstrates a transfer function measurement made on the same system under more realistic conditions: noise is present.

To characterize the measurement noise, the system's excitation was set to zero. Figure 3 shows a snapshot of a time history (upper plot), and spectrum (lower plot) of the measured system response $y_m(t)$. Since the system's input is zero, this is the noise $n_y(t)$ in Figure 1.

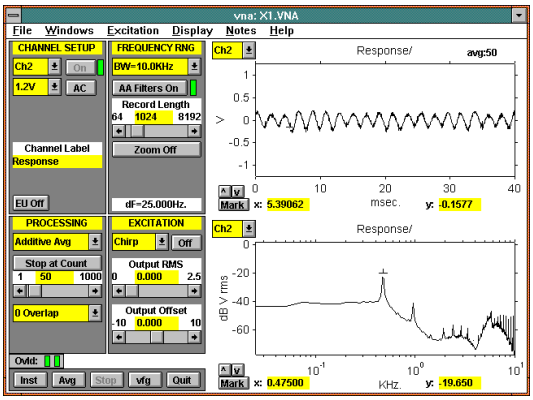

Figure 3 - Noise time history $n_y(t)$ and its power spectrum.

Fifty frequency-domain averages were used to estimate the noise spectrum. It can readily be seen that the resulting spectrum in the lower plot is not white, i.e. not flat. The noise is a combination of both random and periodic components. This noise spectrum is similar to what might be found in disk drive head positioning servo system.

Figure 4 shows the effect of this noise on the transfer function estimate. It is clear that the magnitude curve is no longer smooth, especially at the lower frequencies, in spite of doing 50 measurement averages. This is five times the amount of averaging done in the previous measurement example.

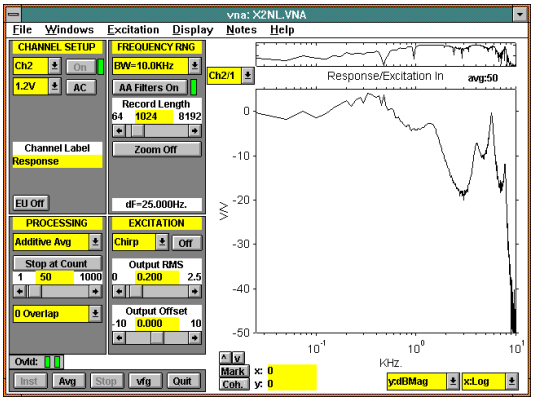

Figure 4 - Transfer function estimate of a noisy system.

The coherence is no longer unity across the measurement band. The coherence is closest to unity where the noise power is minimal and the system response to the excitation is

high. The sharp dips in the coherence occur where there is significant power from the periodic noise components.

For a linear system, there are two ways to improve the measurement: increase the system excitation level or increase the amount of averaging.

Figure 5 is the transfer function estimate under identical operating conditions but with 1000 averages. The acquisition, processing, and averaging took about 40 seconds to complete. There is a clear improvement in the transfer function estimate over the estimate in Figure 4. Notice however that aside from being a smoother curve, the coherence has not changed significantly. The noise has not been lowered nor the excitation increased, therefore the coherence has not improved. The important point is, that in spite of the low coherence, the transfer function measurement has converged quite nicely to the estimate made in Figure 2.

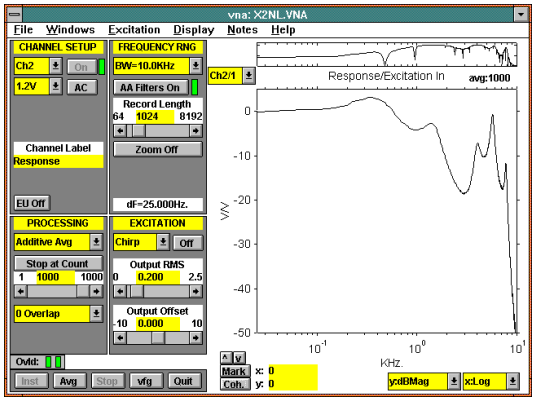

Figure 5 - Transfer function estimate with 1000 averages.

Due to the construction of this particular system, increasing the excitation level is not an option. The system becomes non-linear with larger input signals and this behavior will be now be discussed.

A non-linear measurement example.

The previous examples provides an idea of how noise in a system affects the transfer function estimate. The affects of non-linearity will now be considered.

First, it is beneficial to understand and quantify the non-linear behavior of the DUT. An assessment of linearity is easy to do if the system is noise-free. Injecting sine waves, possibly at multiple frequencies, and using spectrum analysis to measure harmonic or intermodulation terms is a common approach.

With the addition of system noise, non-linear behavior becomes more difficult to quantify. For example, Figure 6 shows a time history snapshot of the system noise (no averaging) along with the power spectrum of the noise computed from 100 frequency domain averages. This data is similar to that shown in Figure 3, but the analysis bandwidth is 20 kHz and a linear x-axis is used for the spectrum plot.

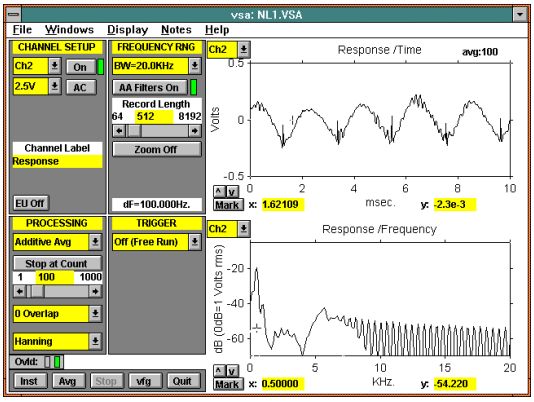

Figure 6 - Response time history and noise spectrum with no excitation.

If a periodic function (such as a sine wave) is used as the system's excitation in the attempt to measure linearity, it is difficult to tell which harmonics are due to the excitation given the many (and possibly large) periodic components in the system noise.

One solution to this problem is to use a triggered mode of data acquisition and average the time histories. For this procedure to work, the trigger source must be synchronized to the fundamental period

of the excitation. SigLab has the ability to generate a variety of periodic excitations. An internal digital signal is produced with a period identical to the chosen excitation period. This signal provides virtually perfect trigger synchronization. The time averaging then reduces, to an arbitrarily small level, the portion of the measured response signal due to the system noise $n_y(t)$ if (and only if) this noise is not correlated with the excitation provided by SigLab. It is therefore important to choose an excitation period that is unrelated to any of the periodic components in the noise.

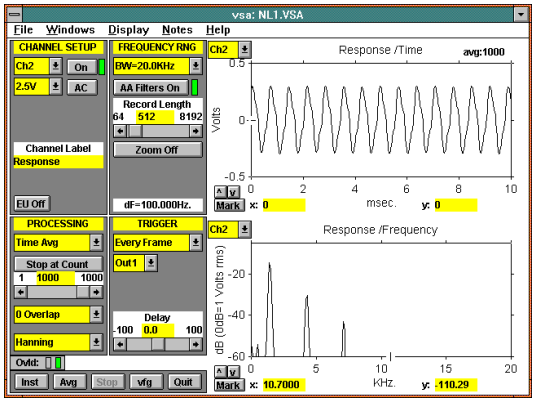

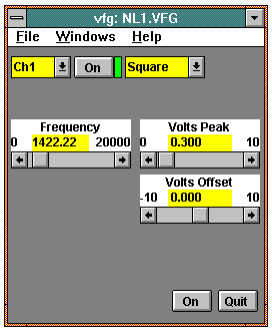

Figure 7 - Time averaging reduces the system noise and enhances the system response to the squarewave excitation specified by the function generator application to the left.

Figure 7 shows the effect of time averaging the system's response. The excitation is a square wave of 0.3 volts peak amplitude (0.6 volts peak-peak). The time history on the upper display is the response of the system to the 1422.22 Hz square wave. Notice that the noise has been reduced to below -60 dB Vrms, except for the component at approximately 500 Hz. Also notice that the DUT is acting like a low pass filter and only the first three components of the square wave excitation are visible in the spectrum plot. The square wave has a perfect 50% duty cycle. Therefore, only the odd harmonics of the fundamental should be present in the spectrum plot. Under the current operating conditions, this proves to be the case.

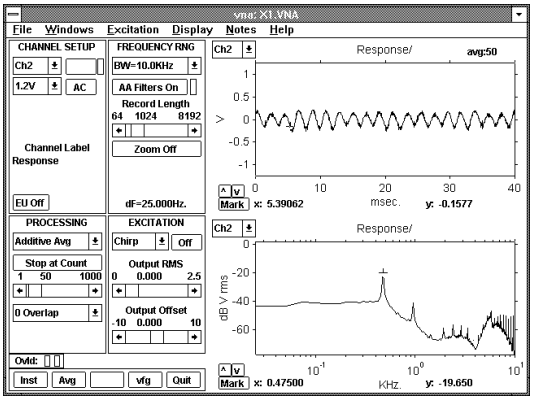

Figure 8 - Increasing the amplitude of the squarewave gives rise to even harmonics of the fundamental frequency, a sign of midly non-linear behavior.

The results shown in Figure 8 are due to increasing the amplitude of the square wave to 0.6 volts peak (1.2 volts peak to peak). The time history has increased in amplitude, and appears to have the same general shape as that of Figure 7. However, the spectrum now clearly shows even harmonics of the fundamental frequency. This is an indication of the system becoming non-linear. The onset of non linear behavior is usually a gradual process. The increases in the even harmonic content could be actually be seen at levels on the order of 0.4 volts peak, but these harmonics are hard to interpret and the quality of the transfer function estimate is not affected significantly by mildly non-linear behavior.

To provide a better idea of the advantage of the synchronous time averaging, Figure 9 shows the same analysis but with frequency domain averaging. The square wave fundamental and the first two odd harmonics can be easily identified, but the random and periodic system noise obscures the even harmonic information.

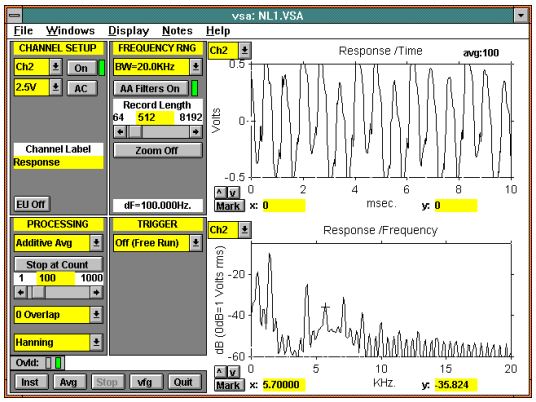

Figure 9 - Frequency domain averaging does not reduce the system noise which obscures the non-linear response of the system.

How does non linear system behavior affect the transfer function estimate?

The concept of the transfer function, as well as its estimation techniques are both based on the assumption that the system being analyzed is linear and time-invariant. When this assumption is violated, it should not be a surprise that errors in the estimation can, and do, arise.

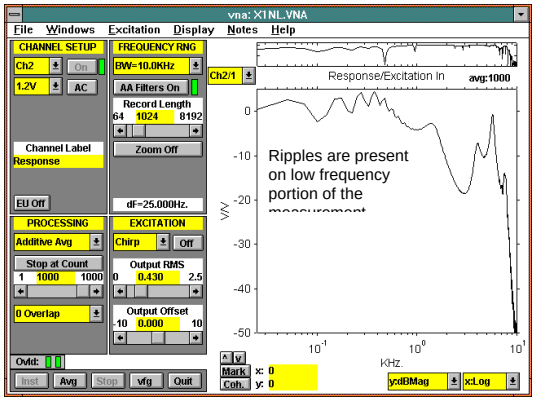

Figure 10 - Transfer function estimate when system is driven into non-linear region.

As shown in Figure 8, the system exhibited mildly non-linear behavior when the peak excitation amplitude reached 0.6 volts. The results of measuring the transfer function with an increased excitation level (0.43 volts rms which is about 0.6 volts peak for the chirp) are shown in Figure 10.

Notice the prominent ripples in the low frequency portion of this measurement.

Because these errors are due to non-linear DUT behavior (not noise), more averaging will not lead to a better measurement.

Also note that the coherence has improved over the results shown in Figure 5. This is due to the increase in excitation amplitude. However, the coherence estimate is also based on linear system assumptions, so even though the coherence is higher, the measurement error is higher than that of Figure 5. Clear evidence that the coherence is not a trustworthy indicator of measurement quality when the system is non-linear.

Measurement results will change with the type of excitation

When the system is non-linear, different types of excitation will typically produce different transfer function estimates. It has just been shown that the transfer function estimate can change with the amplitude of the excitation (the low frequency errors were higher at increased excitation levels).

Inconsistent transfer function estimates also provides another clue that the system is non-linear. If the DUT were perfectly linear, all types of excitations and excitation levels would produce consistent transfer function measurements.

The chirp has three nice properties when used as an excitation for FFT based techniques. First, it is easy to construct the chirp so its spectral energy lies exactly on the analysis lines of the FFT. This removes the requirement of using a window with the FFT, therefore better frequency resolution can be obtained for a given record length. Second, the crest factor (ratio of peak to rms. voltage) is $\sqrt{2}$ which is relatively low. This should allow the DUT to be driven at a higher rms level than random noise before clipping occurs. Third, its time derivatives are continuous so it is often a more gentle

well behaved excitation for mechanical systems.

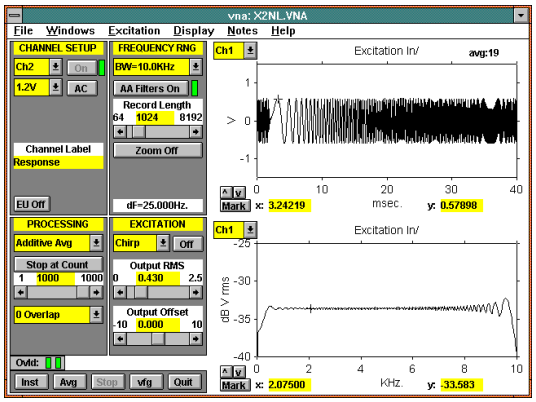

Figure 11 - Time history and spectrum of the chirp excitation.

Figure 11 shows a time history of the chirp along with its spectrum. The chip repeats every input acquisition frame, which is set at 1024 samples. When the chirp is constructed to repeat every N samples, its energy must lie at discrete frequencies. This is a result of basic Fourier analysis. The period of the chirp repetition is then N/F_S where F_S is the sampling frequency. SigLab always samples at a rate equal to $2.56 \cdot Bandwidth$, therefore, for an analysis bandwidth of 10 kHz, and a 1024 point input frame, the underlying period is 40 ms. The reciprocal of 40 ms is 25 Hz thus excitation energy is provided at 25, 50, 75, 100, ... 9975 ,10000 Hz. Note that the chirp's peak level is slightly less than 0.6 volts.

Random noise excitation is also a popular broad-band stimulus. Of course, the random excitation is actually a very long pseudo-random sequence. When SigLab is set to the 10 kHz bandwidth, the sequence repeats every 46 hours. It is therefore, for all practical purposes, random. Unlike the repetitive chirp, the random sequence has a virtually continuous energy vs. frequency distribution, therefore, to minimize leakage effects, a windowed FFT is typically required. Random also has a higher crest factor than the chirp, so the peak excursions are higher than the chirp for the same rms level. Note that Figure 12 shows peaks over 1.2 volts in amplitude for the 0.43 volt rms output.

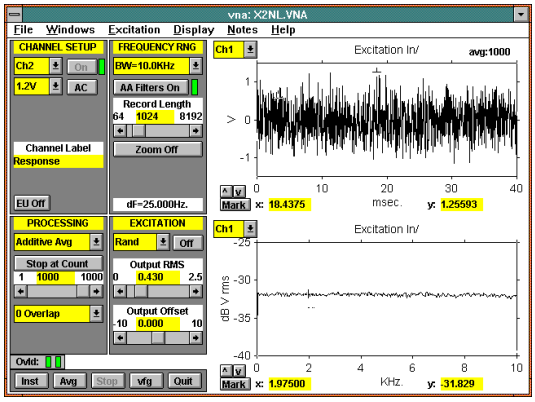

Figure 12 - A random excitation produces a higher peak-to-peak voltage over that of the chirp for the same rms level.

Since non-linear behavior has been exhibited by this system at high excitation amplitudes, it is reasonable to expect that the random excitation will provide poorer measurements (with respect to the chirp) due to its higher peak excursions.

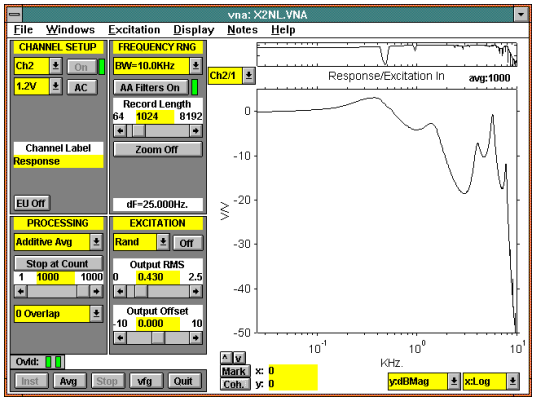

Figure 13 - A random excitation produces a better measurement than the chirp for this particular system.

Actually, the random excitation provided a decidedly better measurement than the chirp! Figure 13 shows a transfer function estimate made with random noise as the excitation. The low frequency ripples in Figure 10 are not present.

Measurements at various nodes within the system revealed that the peak response levels occurring with random excitation were lower in amplitude with the random when compared to the the chirp excitation. So in spite of the instantaneous peak levels of the random excitation being about 2:1 greater than the chirp, the internal signals in the system stayed at lower peak levels and within a linear range. The chirp managed to get significant energy into the system's high-Q resonances and non-linearity became an issue. The chirp can be viewed as a sweeping sine tone. If the tone frequency is at or near a resonance of the system for a significant period of time, the response of this resonance will build in amplitude. The random sequence is naturally highly uncorrelated and therefore the amplitudes of the response were less than with the chirp.

Swept-sine: when the going gets tough

Up to this point, good accuracy has been obtained with the broad-band FFT based transfer function measurements. When the noise and non-linearity are extreme, swept-sine is the tool of choice for three reasons. First, a sinusoidal excitation feeds the most energy possible at a given measurement frequency into the system. Second, the use of tracking filters reduces the unwanted affects of noise on the measurement. Third, the swept-sine technique gives the most flexibility to tailor the measurement to the DUT.

The swept-sine application allows the user to decompose the overall analysis range into from one to five sub-ranges called spans. In each of these spans the acquisition, analysis and stimulus parameters can be optimized to tradeoff measurement speed, frequency resolution, and/or accuracy.

Unlike the FFT approach, the swept-sine application can make frequency response measurements at logarithmically spaced frequency points. Figure 14 shows the swept-sine application and the measurement results. Note that the rms level of the excitation was set to one-half the value used in the FFT based measurements. In fact, due to the previously mentioned system responses to the chirp at resonances, a higher amplitude could lead to a decrease in the measurement quality. The frequency spacing of the measurements was set to be logarithmic. The total measurement time for 85 different frequency points was 6 minutes and 20 seconds. The measurement was made using 3 spans—each with different tracking filter bandwidth, averaging, and logarithmic frequency step size. Different excitation levels for each span could have also been specified, but were not.

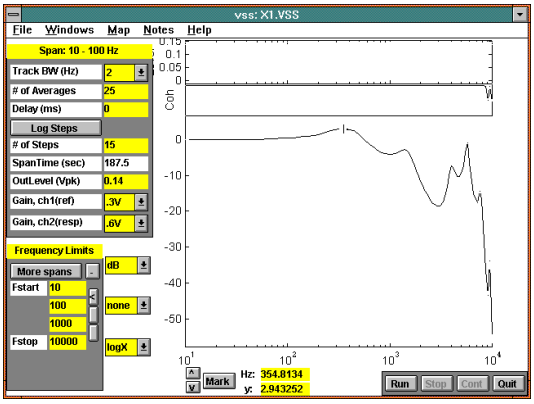

Figure 14 - The swept-sine technique measures the transfer function with a lower excitation amplitude at the expense of measurement time.

Therefore, in spite of the noise and non-linearity, the swept-sine produced an excellent measurement using only half the excitation drive level of the previous measurements.

Measurements of Control Systems

The measurement motivation

Transfer function estimation is virtually mandatory in control systems engineering. The following are the three most common transfer function measurements made on control systems:

1. Overall open-loop response (stability analysis)
2. Plant dynamics (plant modeling)
3. Closed-loop response (system performance)

Often these measurements must be made on the control system under actual operating conditions. For example, many plants contain an intrinsic integrator making their operating point difficult to stabilize. During the early stages of development, it is a common practice to construct a simple controller to stabilize the operating point of the plant. This allows the dynamics of the plant to be studied in greater detail. Subsequently, when the controller design is refined, measurements again need to be taken to fully characterize the overall system, not just the plant.

To make the closed-loop response measurement, no special techniques beyond those previously discussed in this note are required. Simply excite the control system at its command input and measure the response. The measurement configuration is shown in Figure 1. The remaining two measurements (open-loop response and the plant dynamics) will be discussed in the following sections.

The physical system

The DUT used in the previous measurement examples is a real physical system. Until this point, it has simply been treated as a mildly non-linear single-input single-output system with measurement noise. In fact, the system that has been measured, is the control system shown in Figure 15 (beneath the broken line). Several measurement configurations were setup with a rotary switch (shown as A, B, C, D below SigLab's inputs). All the previous measurement examples were made with the selector in the B position. This control system hardware will be explored in the remaining measurement examples.

The complete control system consists of the controller and plant. The plant is a single input single output system with impulse response $h(t)$. The controller is a two input single output system. The output of the controller is a linear combination of the command input and the position input from the plant. The command and position inputs are convolved with the controller dynamics represented by $c(t)$ and $g(t)$, and the difference is taken to produce the controller output $y_{gh}(t)$. The equation for this operation is shown inside the controller block. The noise due to the normal operation of the control system loop is represented by $n_R(t)$. The noise source, $n_R(t)$, is actually another SigLab generating a combination of a periodic sawtooth and bandlimited random disturbance.

In the disk drive scenario this noise signal would be due to imperfections in the servo track, platter or track eccentricity, spindle bearing imperfections, or other mechanical errors. Therefore, in the real world, the user has little or no control over this error source. For the purposes of this note, the error source can be turned off when desired. This allows a comparison to be made between measurements with and without noise.

It is a common practice to add a summing circuit in the feedback loop of the control system. This allows the measurement instrumentation to inject a signal into the system. In this example the summing circuit is between the controller output $y_{gh}(t)$ and the plant command input $u(t)$. The exact position of this circuit in the control loop may vary from design to design but the principles to be discussed are not changed significantly.

Measurement configurations

Figure 15 shows a switch which can select one of four typical control system measurement configurations. This switch is not usually present in an actual test setup, but it is shown here to allow a comparison of several possible measurement configurations.

It should be noted that position A of the selector switch is the only configuration of the three that does not satisfy the requirement that the excitation be measured directly by SigLab per Figure 1. The other configurations (B, C, D) meet this requirement will therefore provide unbiased transfer function measurements.

Notation

The following discussion will use notation where upper case letters refer to the continuous time Fourier transform of the signal as in (3a) and (3b).

$$X(w) = \mathcal{F}(x(t)) \qquad (3a)$$

$$G(w) = \mathcal{F}(g(t)) \qquad (3b)$$

For all the examples, the equations were written in terms of w, but the display results are in terms of f where $f = w/2p$.

Configuration A: direct estimate of the open-loop transfer function using the broad-band FFT analyzer

Measuring the open-loop response of a control system is a common requirement. This measurement information is important in assessing the stability of the loop. The open-loop transfer function $G(w)H(w)$ can be measured directly by selecting switch

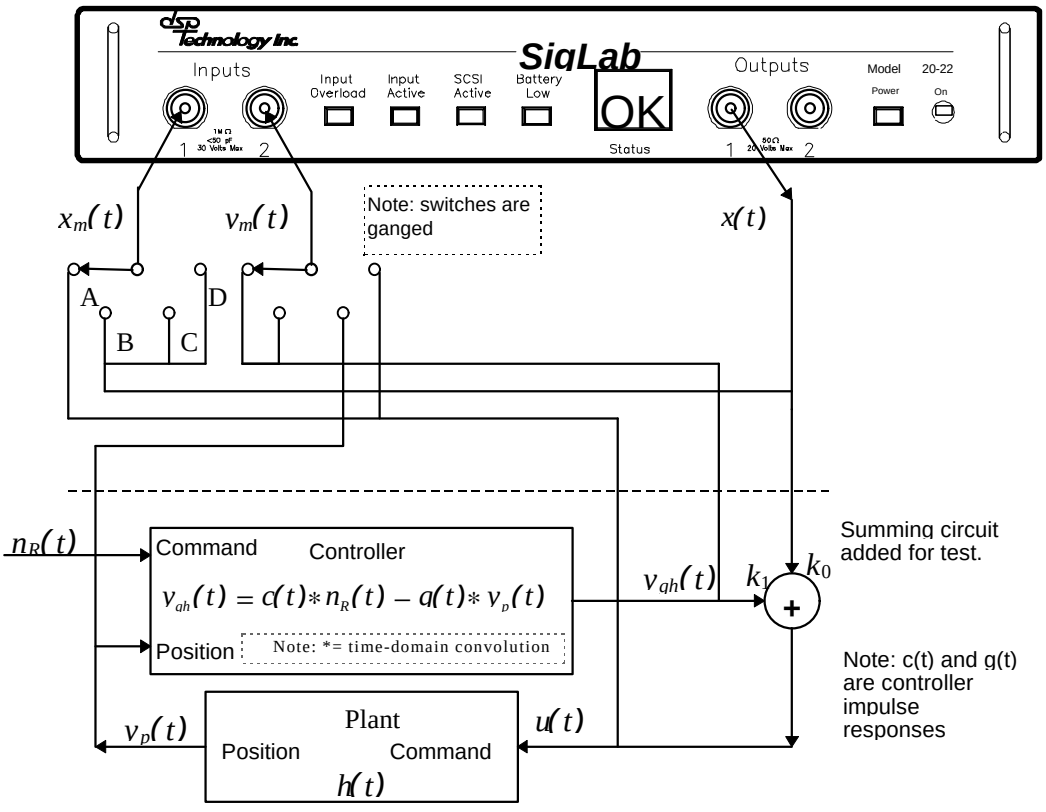

Figure 15

position A. This connects plant input $u(t)$ to SigLab channel 1 and the controller response $y_{gh}(t)$ to SigLab channel 2. Excitation to the overall system is provided by feeding $x(t)$ into the summing amplifier. The advantage of this configuration is the measurement of the open-loop transfer function is made directly. No detailed understanding or inclusion of the parameters of the test summing circuit is required. The approach is intuitively appealing due to its simplicity.

It is important to note that the excitation signal $x(t)$, is not being measured by SigLab, and therefore, the estimator given by (1) will yield a *biased* transfer function estimate due to the noise source $n_R(t)$. If, however, $n_R(t)$ is negligible, the transfer function can be estimated with (1) without significant error. Other connection variations are possible such as measuring between the plant input $u(t)$ and output $y_p(t)$ but the results will be similar to results obtained using switch position A.

Figure 16 shows the result of this direct measurement in a noise free situation (where $n_R(t)$ is set to zero). The resulting transfer function data will be viewed as being the true open-loop transfer function of the system.

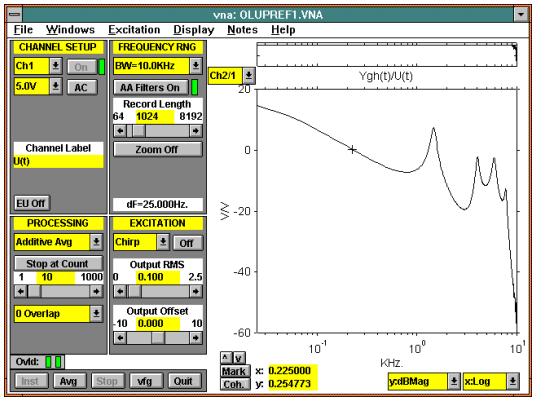

Figure 16 - The open-loop response measured directly under noise free conditions.

Now, the measurement will be repeated, but the noise source will be reactivated and set to the level used in the measurements shown in Figure 5.

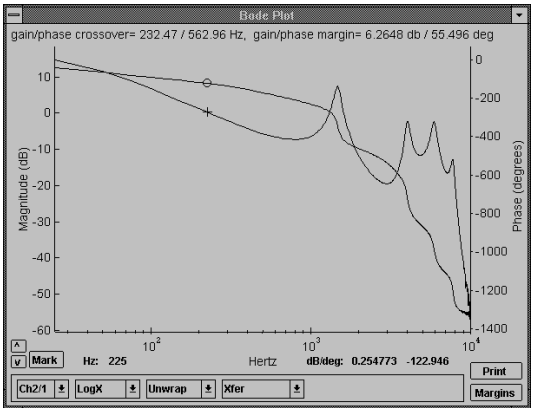

Figure 17 - Direct open-loop measurement with noise.

A visual comparison between Figure 16 and Figure 17 indicates that a nearly 15 dB measurement error exists at low frequencies. Using a few simple MATLAB commands the magnitude difference in dB between the two measurements may be plotted. This error is shown in Figure 18.

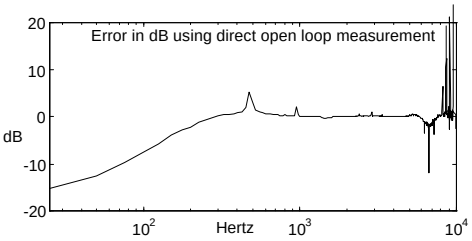

Figure 18 - Estimation error using the direct open-loop measurement when noise is present.

One thousand measurement averages were used to compute the transfer function estimate in Figure 17. The coherence looks deceptively good. The fact is, this measurement cannot be improved by any increase in averaging because it is a biased measurement. Due to the system's non-linear behavior, the excitation level cannot be increased.

The underlying problem is the estimator defined in (1) cannot be successfully used since there is significant noise in both the

excitation measurement $x_m(t)$ and the response measurement $y_m(t)$. To make matters worse, the measurement noise on these two input channels is correlated since this noise is a result of the single noise source $n_R(t)$. Here is a case where the usual measurement quality indicators (good coherence and the smooth, credible transfer function magnitude) all point to a good measurement, but, since the assumptions of Figure 1 were not observed, the measurement is seriously flawed.

Configuration A: direct estimate of the open-loop transfer function using swept-sine analysis

There are ways, however, to combat this correlated noise. Of course, nothing is free: it costs measurement time and there is risk of error. As previously discussed, the swept-sine technique uses tracking band-pass filters on the measurement channels. As the bandwidth of these tracking filters is reduced, the effect of noise $n_R(t)$ is minimized on both measurement channels. If $n_R(t)$ is a broad-band signal, it is easy to see how this filtering can improve the measurements.

Often, however, $n_R(t)$ contains large periodic components e.g. at multiples of the platter rotational speed in the case of disk drives. In this case, the user must either carefully structure the measurement so that these noise components do not lie within the tracking filter bandwidth at the desired measurement frequencies, or accept reduced accuracy at frequencies where they do.

The results of using the swept-sine technique are shown in Figure 19. This measurement is in good agreement with that of Figure 16 except for the spike at around 9000 Hz due to a harmonic of the periodic component of the noise.

It should be recognized that the swept-sine technique also relies on the estimator given in (1). The tracking filters and single frequency sine excitation often allow good measurements to be made even when the assumptions of linearity and noiseless input measurements are invalid. Since the coherence estimate (2) is based on the same measurement assumptions, it is also suspect. However, the largest single disadvantage of the swept-sine technique is that of measurement time. As the tracking filter bandwidth is reduced to improve the measurement, the measurement time naturally increases. For example, this particular measurement took over 5 minutes to complete.

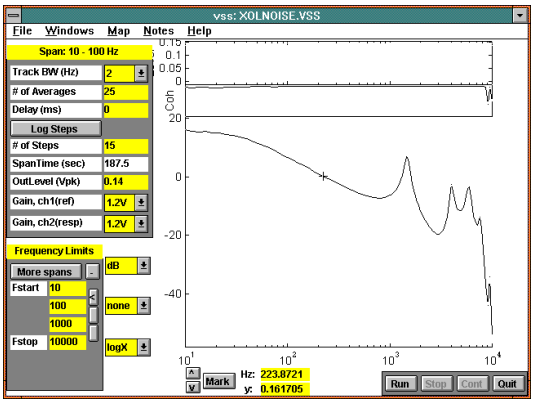

Figure 19 - Swept-sine's digital tracking filters can be used to reduce the effect of the noise on the input channels.

Configuration B: estimating open-loop dynamics from a closed-loop measurement.

A popular alternative method to directly measuring the open-loop transfer function involves making an unbiased transfer function measurement of the closed-loop response which relates $y_{gh}(t)$ and $x(t)$.

This estimate is then mapped (or transformed) to the open-loop transfer function. With the selector switch in position B, the following equation relating $y_{gh}(t)$ and $x(t)$ in the frequency domain may be written:

$$Y_{gh}(w) = \frac{N_R(w)C(w)}{1+G(w)H(w)} - \frac{X(w)G(w)H(w)}{1+G(w)H(w)} \quad (4)$$

This equation assumes the test summer has gains of $k_0 = k_1 = 1.0$

Examining (4) shows that the response $Y_{gh}(w)$ contains a noise term due to the system operation $N_R(w)$ and a term due to the excitation $X(w)$. This is the same situation as shown in Figure 1 but in frequency domain terms: e.g. the system response is corrupted by additive noise that is not necessarily white or random. Again, for the resulting transfer function to be unbiased, the only underlying measurement assumption is that the noise is uncorrelated with the excitation.

If the transfer function relating $Y_{gh}(w)$ and $X(w)$ is measured, a simple mapping will provide the open-loop transfer function $G(w)H(w)$.

First, let the measured transfer function be defined as:

$$T(w) = \frac{Y_{gh}(w)}{X(w)} \quad (5)$$

Then:

$$G(w)\cdot H(w) = \frac{-\frac{1}{k_1}\cdot T(w)}{\frac{k_0}{k_1} + T(w)} \quad (6)$$

In the mapping given by (6), the summing circuit gain constants (k_0, k_1) are now included as variables.

For the best mapping results, it is important to accurately know the values of these constants. The denominator term $\frac{k_0}{k_1}$ is particularly important, since often there are one or more integrators in the loop. This forces

$$\lim_{w \to 0} T(w) = -\frac{k_0}{k_1}$$

Therefore, at low frequencies, the estimated open-loop transfer function is a sensitive function of the above ratio.

Since the transfer function estimate of $T(w)$ is unbiased, this simple mapping (closed to open-loop) provides an unbiased method of estimating the combined controller and plant dynamics.

Figure 20 may look familiar. It is the same measurement that was made in the initial part of the this note. This measurement is now referred to as the closed-loop transfer function $T(w)$.

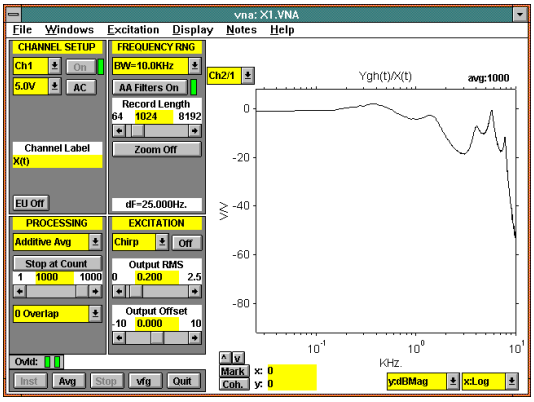

Figure 20 - Closed-loop transfer function measurement $T(w)$.

Control systems engineers often need to display both the magnitude and phase of the transfer function in a Bode plot format shown in figure 21. With simple point and click operations, the SigLab software performs the mapping in (6), displays the results in the Bode format, and displays gain and phase margins.

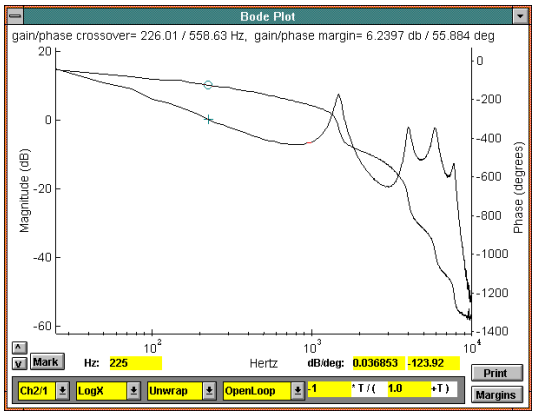

Figure 21 - Bode plot of closed to open-loop mapping with gain and phase margins.

The open-loop transfer function computed by mapping the closed-loop measurement is in excellent agreement with the direct (noise-free) measurement made in Figure 16. The mapping technique is popular because it provides a trustworthy estimate of the open-loop transfer function with minimal effort.

Configuration C and D: estimation of the plant transfer function from two measurements.

Often, a measurement of a single section of the control system is desired. For instance, the plant transfer function $H(w)$ is commonly required as input data for frequency domain system identification. If the controller dynamics, $G(w)$, are known, a division will provide $H(w)$ from the open-loop function . However, a direct measurement of $H(w)$ is still often preferable. As previously shown, the swept-sine technique can sometimes be used with success to make measurements that violate the requirements in Figure 1, but this is risky business.

A two-step measurement procedure is a good is approach for measuring the plant dynamics. With the switch in Figure 15 in the C position, the output of the plant $y_p(t)$ is being measured by SigLab's channel 2 and the excitation into the test summing circuit $x(t)$ by SigLab's channel 1. If a transfer function estimate is made, it will be unbiased since this excitation is being measured. Define this transfer function and coherence measurement as: $\hat{H}_{YX}(w)$ and $\hat{C}_{YX}(w)$ respectively.

With the switch in position D another unbiased transfer function estimate can be made relating the excitation $x(t)$ and plant input $u(t)$. This transfer function and coherence measurement is defined as: $\hat{H}_{UX}(w)$ and $\hat{C}_{UX}(w)$ respectively.

These independent unbiased estimates can be combined to provide an unbiased estimate of the plant transfer function (7)

$$\hat{H}(w) = \frac{\hat{H}_{YX}(w)}{\hat{H}_{UX}(w)} \qquad (7)$$

as well as an composite coherence (8).

$$\hat{C}(w) = \hat{C}_{YX}(w) \cdot \hat{C}_{UX}(w) \qquad (8)$$

The advantage of this technique over attempting to measure the plant directly (e.g. relating $u(t)$ and $y_p(t)$ while ignoring $x(t)$), is that the estimates will be unbiased and therefore with sufficient averaging converge to the correct results.

If three measurement channels are available, the two transfer function estimates can be made simultaneously. In fact, by writing (7) and (8) in terms of (1) and (2), the result is yet another transfer function estimator:

$$\hat{H}(w) = \frac{\hat{P}_{xy}(w)}{\hat{P}_{xu}(w)} \qquad (9)$$

and composite coherence indicator:

$$\hat{C}\ (w) = \frac{\left|\hat{P}_{xy}(w)\right|^2 \cdot \left|\hat{P}_{xu}(w)\right|^2}{\left|\hat{P}_{xx}(w)\right|^2 \cdot \hat{P}_{yy}(w) \cdot \hat{P}_{uu}(w)} \qquad (10)$$

Using a three channel simultaneous measurement, the measurement speed will double and the end result will be a bit more accurate, but three channels are not mandatory.

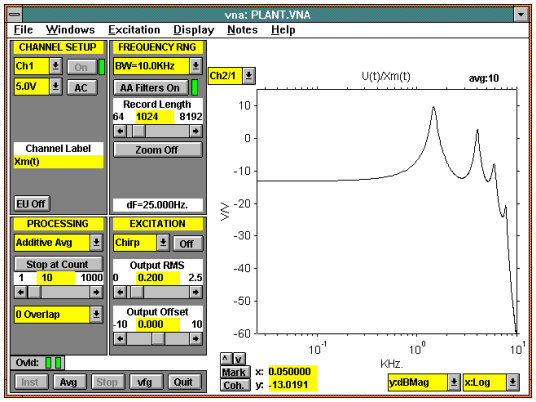

Figure 22 - Plant transfer function $H(w)$.

In order to verify the previous dual transfer technique, a noise free measurement of the plant is made. Since measurement noise can be eliminated (for this example), the plant transfer function can be accurately measured by the direct means. The transfer function is shown in Figure 22.

Now, the task is to estimate the plant transfer function under the same conditions that were present (noise and non-linearity) for the open-loop measurement using (7) and (8). Since SigLabs can be combined to create multi-channel systems, two SigLabs were linked for the following measurements.

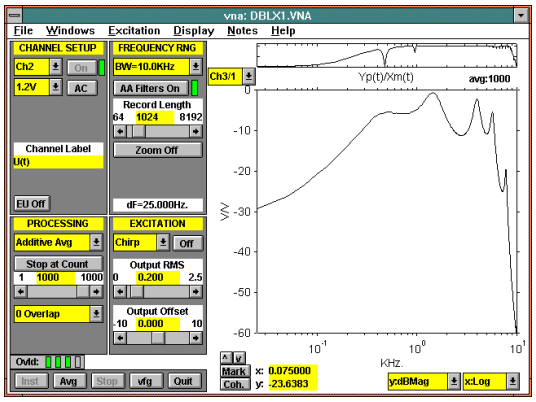

Figure 23 - Transfer function $\widehat{H}_{YX}(w)$, ***corresponding to switch position C.***

The two transfer function configurations correspond to switch positions C and D. Figure 23 shows the $\widehat{H}_{YX}(w)$ transfer function estimate made with the switch in the C position. Note that the coherence is close to zero at the low frequency end of the measurement. However, since the measurement is unbiased, it will converge to the actual transfer function given sufficient averaging. Even with 1000 averages, SigLab took less than one minute to complete this measurement.

Figure 24 shows the second transfer function measurement now made with the switch in position D. The coherence in this measurement is also very low at low frequencies.

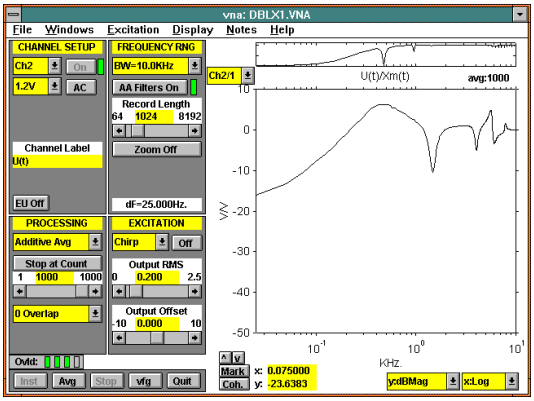

Figure 24 - Transfer function $\widehat{H}_{UX}(w)$, ***corresponding to switch position D.***

The simple MATLAB script file in Listing 1, was used to compute and plot the plant transfer function estimate $\widehat{H}(w)$.

The resulting plant transfer function plot is shown in Figure 25. A comparison between Figure 22 and 25 shows the excellent agreement between the plant transfer function estimate using (9) and the plant transfer function which was measured directly in Figure 22. To get a closer look at the difference between $\widehat{H}(w)$ and the $H(w)$ script M-file was extended to compute and plot the magnitude (in dB) difference between the measurements.

```
% M-file dual_x.m
load dblx1.vna -mat
% this is a 3 channel meas
H=XferDat(:,2)./XferDat(:,1);
% the plant transfer function
Coh = CohDat(:,2).*CohDat(:,1);
% composite coherence

semilogx(Fvec,20*log10(abs(H)),...
         'color','white');
axis([25,10000,-50,10]);
title('Plant transfer function');
xlabel('Hertz');
ylabel('dB');
%
```

Listing 1 - M-file script computing $\widehat{H}(w)$.

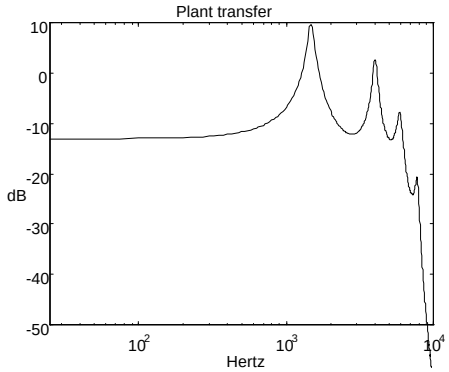

Figure 25 - Plant transfer function estimated on a non-linear and noisy system by the method in Listing 1.

The error is plotted in Figure 26. There is excellent agreement between this estimate and the actual plant, even at the low frequencies where the coherence of the estimator is almost zero. The errors increased at the high frequency end of the measurement where the plant response is rapidly rolling off. This of little concern since it is well beyond the interesting dynamics of the plant.

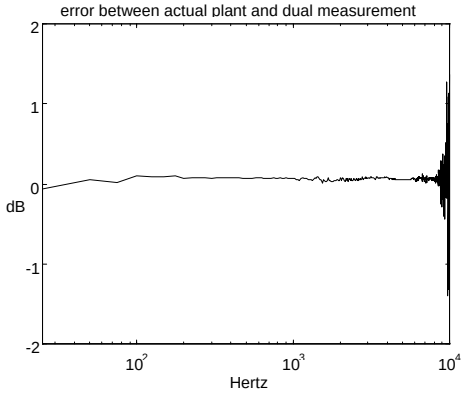

Figure 26 - Magnitude difference between $\widehat{H}(w)$ and $H(w)$.

The composite coherence is also easy to compute and it is plotted in Figure 27. Note the dips due to the periodic components in the noise $n_R(t)$. These coherence and transfer function estimates can serve as the input to frequency domain identification algorithms.

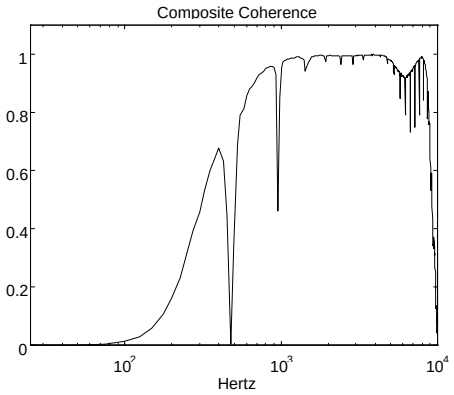

Figure 27 - Composite coherence calculation from Listing 1.

Conclusion

Making transfer function estimates on noisy non-linear systems is far more difficult than in the noise-free, linear case. A high quality measurement can be obtained even under adverse conditions, by using either the closed to open-loop mapping techniques, or by making two unbiased transfer function estimates and combining them. The measurement setup and assumptions outlined in Figure 1 should be observed for optimal results.

Although the bulk of the examples presented used the broad-band FFT based estimation technique, the swept-sine analysis will do as well or better. If the measurement results are suspect using the broad-band FFT technique, it is prudent to repeat the measurement with swept-sine to get a different measurement viewpoint. If a meaningful transfer function exists, swept-sine will do the job when all else fails.

For more information contact:
Spectral Dynamics
1010 Timothy Drive
San Jose, CA 95133-1042
Phone: (408) 918-2577
Fax: (408) 918-2580
Email: siglabsupport@sd-star.com
www.spectraldynamics.com

---

[1] Welch, *The use of Fast Fourier Transform for the Estimation of Power Spectra: A Method Based on Time Averaging over Short Modified Periodograms*, IEEE Transactions on Audio and Electroacoustics, vol AU-15, June 1967, pp. 70-73.

see also

T. P. Krauss, L. Shure, J. N Little, *Signal Processing Toolbox Users Guide*, The MathWorks, pp 1-72 - 1-73, June 1994.

Printed in U.S.A.